symmetry

MDPI

Article

The Role of Hidden Symmetry in Inertial Instability Dynamics

Diana-Corina Bostan [1], Adrian Timofte [1,*], Florin Marian Nedeff [2,*], Valentin Nedeff [3], Mirela Panaite-Lehăduş [2] and Maricel Agop [4,5]

[1] National Meteorological Administration, Bacău Regional Forecast Center, Timpului Street, No 3, 600234 Bacău, Romania; dianabostan06@gmail.com
[2] Department of Environmental Engineering, Mechanical Engineering and Agritourism, Faculty of Engineering, "Vasile Alecsandri" University of Bacau, 157, Calea Marasesti, 600115 Bacau, Romania; mirelap@ub.ro
[3] Department of Industrial Systems Engineering and Management, Faculty of Engineering, "Vasile Alecsandri" University of Bacau, 157, Calea Marasesti, 600115 Bacau, Romania; vnedeff@ub.ro
[4] Department of Physics, Gheorghe Asachi Technical University, Bd. Dimitrie Mangeron 67, 700050 Iasi, Romania; m.agop@yahoo.com
[5] Academy of Romanian Scientists, 3 Ilfov, 050044 Bucharest, Romania
* Correspondence: timofte.adrian@gmail.com (A.T.); florin_nedeff@ub.ro (F.M.N.)

Abstract

Inertial instability is a key process in the dynamics of rotating and stratified fluids, which arises when the absolute vorticity of the flow becomes negative. This study explored the nonlinear behavior of inertial instability by incorporating a hidden symmetry into the equations of motion governing atmospheric dynamics. The atmosphere was modeled as a complex system composed of interacting structural elements, each capable of oscillatory motion influenced by planetary rotation and geostrophic shear. By applying a symmetry-based framework rooted in projective geometry and Riccati-type transformations, we show that synchronization and structural coherence can emerge spontaneously, independent of external forcing. This hidden symmetry leads to rich dynamical behavior, including phase coupling, quasi-periodicity, and bifurcations. Our results suggest that inertial instability, beyond its classical linear interpretation, may play a significant role in organizing large-scale atmospheric patterns through internal geometric constraints.

Keywords: inertial instability; nonlinear behaviors; *SL(2,R)* group; Riccati equation; symmetry

Academic Editors: Calogero Vetro and Sergei Odintsov

Received: 19 March 2025
Revised: 19 June 2025
Accepted: 21 June 2025
Published: 24 June 2025

Citation: Bostan, D.-C.; Timofte, A.; Nedeff, F.M.; Nedeff, V.; Panaite-Lehăduş, M.; Agop, M. The Role of Hidden Symmetry in Inertial Instability Dynamics. *Symmetry* **2025**, *17*, 994. https://doi.org/10.3390/sym17070994

1. Introduction

Radiative, chemical, and dynamic processes in the atmosphere contribute to shaping the Earth's climate. The Sun heats the Earth unevenly, with more energy reaching the equator than the poles. This causes a net energy gain (positive deviation) at low latitudes and a net loss (negative deviation) at high latitudes. To balance this, energy is transferred from the equator toward the poles by winds and ocean currents. Even though the net energy at the poles is negative (when averaged over the year), the actual amount of solar energy received is still a positive number—just smaller than what is lost. This is a subtle point: the deviation can be negative, but the incoming solar flux is always greater than zero.

The general circulation of the atmosphere, by converting potential energy into kinetic energy, supports this transfer and is influenced by several factors, such as the vertical stratification of the atmosphere, the differential heating of oceans and continents, the presence of mountain ranges (e.g., the Alps, Himalayas, and Rocky Mountains), which

disturb the zonal flow and generate significant tropospheric disturbances, and the curvature of the Earth, which shapes global wind patterns and circulation cells [1].

Inertial instability constitutes one of the fundamental forms of atmospheric instability; it occurs in contexts where rotational forces are no longer balanced by the local distribution of mass and vorticity. It emerges when the velocity gradient or the configuration of the potential vorticity (PV) field leads to a spontaneous redistribution of angular momentum within the air mass, particularly in weakly stratified environments or at low latitudes. In contrast to baroclinic instability—classically associated with the development of extratropical cyclones and meridional energy transport—inertial instability is more localized in nature and is inherently linked to the conservation of angular momentum in a rotating system [2,3].

The general circulation of the atmosphere is described by the existence of three main atmospheric circulation cells: the Hadley cell, which covers the area between the equator and approximately 30–40° latitude and is responsible for the trade winds that carry warm and humid air; the Ferrel cell, located between 30° and 60° latitude, which mediates the transfer of air between the subtropical and polar regions; and the Polar cell, situated between 60° and the poles, where cold air descends toward the surface and moves toward lower latitudes [4–6] (see Figure 1).

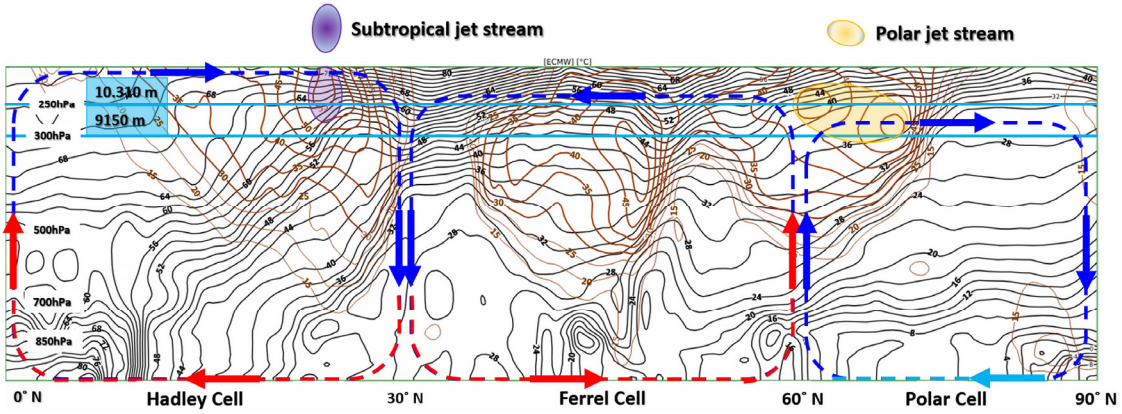

Figure 1. Representation of Hadley, Ferrel, and Polar cells using cross-section from Equivalent Potential Temperature and Isotach map for 1°23′ S 0°13′ W–84°12′ N 0°13′ W (valid 31 January 2025 15:00).

Within the general circulation of the atmosphere, inertial instability plays a subtle yet essential role in the generation and maintenance of coherent structures in the atmospheric flow field. It contributes to the redistribution of momentum in tropical and subtropical regions, thereby influencing the dynamical balance between the Hadley, Ferrel, and Polar cells. Moreover, under extended nonlinear regimes, inertial instability may facilitate the emergence of inertial-gravity waves and quasi-periodic modes that modulate the large-scale structure of atmospheric circulation [2–6].

Figure 1 [7] illustrates the general circulation of the atmosphere in a meridional cross-section, highlighting the three main cells: the Hadley, Ferrel, and Polar cells. The vertical and horizontal air motions within these cells, indicated by the arrows in the figure, are associated with variations in geostrophic wind and thermal gradients. In the transition zones, where the geostrophic wind shear is strongest (e.g., near jet streams), the ideal conditions for inertial instability can arise.

Thus, the global atmospheric circulation represents a dynamic and interdependent system that regulates the transfer of energy and momentum on a planetary scale. Although

the theory of general circulation has made remarkable progress, numerous questions remain regarding the integration of moist processes and their impact on the global climate.

Inertial-gravitational instability contributes significantly to the organization of atmospheric motions, especially under strong horizontal shear in a rotating frame. This instability, governed by imbalances between Coriolis effects and geostrophic shear, can be captured by simplified local models, which we further explore through the lens of symmetry and synchronization [8–12].

Baroclinic and barotropic instabilities are well-known mechanisms for the generation and development of eddy motions in the Earth's atmosphere. Recent studies have used advanced methods, such as Rossby wave analysis [13], the Galerkin method [14], and Lyapunov–Arnold analysis [15], to better understand these phenomena. Although several theories have been proposed to explain the evolution of atmospheric instability, the research field still faces significant challenges from both theoretical and observational perspectives. [2,3].

In the present study, using an extension of the single-particle model based on a hidden symmetry of the equation of motion, we analyzed the implications of this symmetry in the context of inertial instability dynamics. Within this framework, quasi-periodic modes emerging from inertial interactions can be related to the large-scale organization of the atmospheric general circulation, particularly in connection with the structural behavior of the Hadley, Ferrel, and Polar cells.

This study explored the dynamics of inertial instability through the lens of a hidden symmetry in the equation of motion, highlighting how this symmetry governs both the frequency and phase synchronization among atmospheric structural units. By extending the single-particle model and employing Riccati- and Stoler-type mathematical transformations, we show that inertial instability can generate complex regimes ranging from damped oscillations to deterministic chaos with direct implications for the stability and global organization of atmospheric circulation. In this context, inertial instability is no longer regarded as an isolated phenomenon, but rather as an emergent mechanism embedded in the dynamic architecture of the atmosphere, which has structural relevance for its behavior at the planetary scale.

2. Materials and Methods

In this study, we extend the classical single-particle approximation by incorporating the implications of a hidden SL(2,R) symmetry in the governing equations of motion. Using Riccati-type differential structures and projective geometry, we investigated emergent behaviors associated with inertial instability in a rotating, stratified atmosphere. These include synchronization phenomena such as phase coupling, quasi-periodic transitions, and bifurcations, which arise from local imbalances in geostrophic shear and vorticity. Unlike traditional models that linearize around balanced flows, our approach captures nonlinear coherence across dynamically distinct atmospheric regions through geometric invariants. By projecting the inertial dynamics onto the SL(2,R) group manifold, we constructed a framework in which symmetry-preserving transformations generate structured transitions between dynamical regimes.

Such an analysis is not isolated. Recent applications of SL(2,R) symmetry in complex fluid systems support the use of this formalism in the context of inertial instability [16]. Moreover, studies such as [17,18] emphasized the foundational role of projective geometry in physics, showing that homographic transformations preserve the structural form of fundamental equations—validating their use in modeling the projective synchronization of dynamically distinct regions within the atmosphere. Rebelo and Winternitz [19] demonstrated that differential equations possessing SL(2,R) symmetry exhibit robust qualitative

features under symmetry-preserving transformations, reinforcing our interpretation of structural coherence as an emergent property governed by the Schwarzian derivative. In addition, the work of Arkani-Hamed, Bai, and Lam [20] illustrated how complex dynamical systems can be embedded within projective geometries and positive structures, offering a contemporary theoretical basis for our application of projective parameters to describe emergent synchronization patterns in inertially unstable flows.

Inertial-gravity waves and Rossby waves (associated with baroclinic instability) can interact within nonlinear systems. In weakly stratified regimes or in the presence of strong vertical shear, hybrid instabilities may emerge. Certain models such as those based on the primitive equations or extended quasi-geostrophic formulations can be employed to analyze the transition between weak baroclinic instability and inertially unstable regimes. All computations were performed using GNU Octave 8.4.0 (Free Software Foundation, Boston, MA, USA), a MATLAB-compatible open-source software.

2.1. Synchronizations/Desynchronizations and Atmospheric Dynamics

By generalizing the inertial motion of a particle moving horizontally in a flow corresponding to a zonal geostrophic basic state with velocity u_g, and assuming that the particle's displacement does not perturb the pressure field, one obtains the equation of motion (1), as detailed in Appendix A [8]:

$$\frac{d^2\delta y}{dt^2} + f\left(f - \frac{\partial u_g}{\partial y}\right)\delta y = 0 \tag{1}$$

which represents the motion of a particle moving horizontally and meridionally in the atmosphere. In our model, we assumed that the atmosphere can be assimilated, both structurally and functionally, into a complex system in which its structural units are in continuous interaction. This relation describes inertial oscillations in a sheared geostrophic flow, where stability depends on the sign of the quantity $f(f - \frac{\partial u_g}{\partial y})$. It is important to note that this formulation addresses inertial instability rather than baroclinic instability, as the latter requires vertical shear $\frac{\partial u_g}{\partial z}$.

Equation (1) models the meridional oscillations of an air parcel under the influence of planetary rotation and shear, which serve as a local representation of such instabilities. Each atmospheric cell can thus be interpreted as an oscillatory unit whose dynamics are governed by this fundamental differential equation.

The Coriolis force influences the winds in the Ferrel cell by causing their deflection, which results in the prevailing westerlies between 30° and 60° latitude. In addition, the polar jet stream influences mid-latitude weather patterns by steering storm systems and affecting temperature contrasts. In summer, its northward shift generally leads to weaker storm activity, while in winter, its southward displacement contributes to more frequent and intense storms, cold spells, and precipitation events [2–4].

Rossby waves, whose propagation is enabled by the variation of the Coriolis parameter with latitude (the so-called β-effect), play an essential role in large-scale atmospheric dynamics. While the β-effect does not generate Rossby waves directly, it allows their existence and provides the restoring force that governs their behavior. In a barotropic environment, where density depends only on pressure, Rossby waves conserve absolute vorticity. In contrast, in a baroclinic environment, where density depends on both pressure and temperature, air parcels conserve potential vorticity under adiabatic and frictionless conditions. These waves are fundamental in the development of mid-latitude weather patterns and in the large-scale transport of energy and momentum in the atmosphere. These waves facilitate the transport of energy and matter between atmospheric regions. Barotropic instability is associated with horizontal variations in flow and contributes to the

transfer of kinetic energy, while baroclinic instability is linked to vertical variations and promotes the conversion of potential energy into kinetic energy. These mechanisms are crucial for the formation of cyclones and atmospheric fronts.

Now, we must mention that Equation (1) originates from a classical inertial instability derivation under the quasi-geostrophic framework [8]. These result from linearizing the motion of a parcel displaced meridionally in a zonal geostrophic shear, using the assumption that vertical motion is negligible compared to horizontal dynamics. While this simplification focuses on horizontal accelerations in a rotating frame, it serves here as a proxy for instability onset, allowing for analytical tractability and symmetry analysis (for details, see Appendix A).

Although Equation (1) is a linear equation, certain nonlinear behaviors may result not from the differential form itself but from symmetries induced by both the structure of the equation and its solutions (we call this a hidden symmetry). Lie symmetries are usually used to obtain analytical solutions of differential equations; their composition under projective mappings (e.g., Riccati flows and Schwarzian derivatives) may induce emergent behavior such bifurcations, period doubling, or intermittent dynamics. This happens in extended dynamical settings, particularly in cases when non-autonomous or connected systems undergo transformations, preserving their symmetry [21,22].

Using the notations

$$\delta y = u, \;\; \Omega^2 = f\left(f - \frac{\partial u_g}{\partial y}\right) > 0 \tag{2}$$

the differential Equation (1) becomes

$$\frac{d^2u}{dt^2} + \Omega^2 u = 0 \tag{3}$$

The most general solution of Equation (3) can be written as

$$u(t) = he^{i(\Omega t+\varphi)} + \overline{h}e^{-i(\Omega t+\varphi)}, \; \mathrm{i} = \sqrt{-1} \tag{4}$$

where $\overline{h}$ is the complex conjugate of h. The quantities h and $\overline{h}$ give the initial conditions, which are not the same for every point in space. More precisely, the various atmospheric structural units corresponding to different points in space are in different states and have different phases. A problem arises: is it possible to give a priori connection between the parameters h, $\overline{h}$ and $e^{i(\Omega t+\varphi)}$ of the various atmospheric structural units at a given time? Since Equation (4) is a solution of Equation (3), it allows us to give an affirmative answer to this problem. Indeed Equation (3) possesses a hidden "symmetry" that can be expressed by the homographic group: the ratio of two solutions of Equation (3) is a solution of Schwartz's equation [16,23–25]:

$$\left(\frac{\tau''}{\tau'}\right)' - \frac{1}{2}\left(\frac{\tau''}{\tau'}\right)^2 = 2\Omega^2 \tag{5}$$

where the symbol "$\prime$" defines the derivative with respect to time.

The homographic transformation connects the analytical solutions of the linear equation with the nonlinear behaviors of the atmosphere.

In the context of this study, it transforms a simple local model into a framework capable of explaining the emergent organization of the global atmospheric circulation, providing a bridge between advanced mathematics (SL(2,R)) and dynamical meteorology.

Equation (5) arises from the ratio of two linearly independent solutions of Equation (3) (which is derived from Equation (1)). This ratio satisfies a Schwarzian differential equation that is invariant under the homographic transformations. Physically,

this captures how phase synchronization between atmospheric structural units occurs in a system with inertial instability, which is governed by a shared underlying pulsation.

This construction implies that structural units (e.g., segments of an atmospheric cell) within the atmosphere as a complex system can interact and synchronize not only through explicit external forces, but also via a shared geometric symmetry. The ratio of the solutions thus becomes an "internal message" of the system, encoding how the relative phases of these structural units evolve over time. If two atmospheric structural units evolve such that the ratio of their solutions remains invariant with respect to a homographic transformation, they are said to be projectively synchronized—their individual evolutions differ, yet remain geometrically coherent.

This approach provides a unified framework for understanding collective oscillation modes, including intermittency, bifurcations, and nonlinear synchronization—phenomena that are experimentally observable in atmospheric, electrical, and optical systems [26–28]. From a practical standpoint, one can envision a network of "atmospheric oscillators" that, although locally governed by linear equations, collectively give rise to complex emergent behaviors—precisely what is observed in jet streams, planetary waves, and stable climate cells.

This equation is invariant under the homographic transformation of $\tau(t)$: any homographic function of τ is itself a solution of Equation (5). As homography characterizes projectivity on a straight line, it can be stated that the ratio of two solutions of Equation (3) is a projective parameter for the set of atmospheric structural units of the same pulsation Ω from a given spatial region.

We can easily construct a convenient projective parameter, which would be in one-to-one correspondence with the atmospheric structural unit. First, we observe a "universal" projective parameter—the ratio of the fundamental solutions of Equation (3):

$$k = e^{2i(\Omega t+\varphi)} \tag{6}$$

Any homographic function of this ratio will again be a projective parameter. Among all the functions, the function

$$\tau(t) = \frac{h + \overline{h}k}{1 + k} \tag{7}$$

has, first of all, the advantage of being specific to each atmospheric structural unit. But not only that, another function

$$\tau'(t) = \frac{h' + \overline{h'}k'}{1 + k'} \tag{8}$$

Is specific to another atmospheric structural unit.

The fact that Equations (7) and (8) are solutions of Equation (5) shows us that there is a homographic relationship between them:

$$\tau' = \frac{\alpha\tau + \beta}{\gamma\tau + \delta} \tag{9}$$

Which, after it is clearly expressed, leads to the group equations [16]

$$h' = \frac{\alpha h + \beta}{\gamma h + \delta}, \ \overline{h'} = \frac{\alpha\overline{h} + \beta}{\gamma\overline{h} + \delta}, \ k' = \frac{\gamma\overline{h} + \delta}{\gamma h + \delta}k \tag{10}$$

In such a framework, Equation (10) is identified with the synchronization group of atmospheric structural units. Through this group, the temporal adjustment of the dynamics of the atmospheric structural units (i.e., the local dynamics) is achieved with the global atmospheric dynamics. In practice, the atmospheric structural units adjust their behaviors

so that they oscillate or vibrate synchronously. The structure of the group is typical of SL(2R), i.e., of the form

$$\left[\hat{B}_1, \hat{B}_2\right] = \hat{B}_1,\ \left[\hat{B}_2, \hat{B}_3\right] = \hat{B}_3,\ \left[\hat{B}_3, \hat{B}_1\right] = -2\hat{B}_1 \tag{11}$$

where $\hat{B}_k$, k = 1, 2, 3 are the infinitesimal operators of the group with the expressions

$$\hat{B}_1 = \frac{\partial}{\partial h} + \frac{\partial}{\partial \overline{h}},\ \hat{B}_2 = h\frac{\partial}{\partial h} + \overline{h}\frac{\partial}{\partial \overline{h}},\ \hat{B}_3 = h^2\frac{\partial}{\partial h} + \overline{h}^2\frac{\partial}{\partial \overline{h}} + (h-\overline{h})k\frac{\partial}{\partial k} \tag{12}$$

This group admits the differential 1- forms (absolutely invariant through the group) [14–16]

$$\omega_0 = i\left(\frac{dk}{k} - \frac{dh + d\overline{h}}{h - \overline{h}}\right), \omega_1 = \overline{\omega}_2 = \frac{dh}{k\left(h - \overline{h}\right)^2} \tag{13}$$

and differential 2-forms (metric):

$$\frac{ds^2}{k_0^2} = \left(\omega_0^2 - 4\omega_1\omega_2\right) = -\left(\frac{dk}{k} - \frac{dh + d\overline{h}}{h - \overline{h}}\right)^2 + 4\frac{dhd\overline{h}}{\left(h - \overline{h}\right)^2} \tag{14}$$

The existence of a parallel transport of angles in the Levi-Civita sense [16], which corresponds to the constraint

$$\omega_0 = 0 \tag{15}$$

which transforms Equation (14) as follows:

$$\frac{ds^2}{k_0^2} = 4\frac{dhd\overline{h}}{\left(h - \overline{h}\right)^2} \tag{16}$$

Constraint (15) corresponds to in-phase synchronization of atmospheric structural unities. Thus, we can explain such a situation.

Let us consider an atmospheric field described by the variables Y^i for which the metric

$$h_{il}Y^iY^l \tag{17}$$

was discovered in an ambient metric space

$$\gamma^{\alpha\beta}dX_\alpha dX_\beta \tag{18}$$

In such a context, the field equations derive from the variational principle:

$$\delta\int Ldv = 0 \tag{19}$$

where dv is the elementary volume, relative to the Lagrange function.

$$L = \gamma^{\alpha\beta}h_{il}\frac{\partial Y^i}{\partial x^\alpha}\frac{\partial Y^l}{\partial x^\beta} \tag{20}$$

In our case, metric (17) is given by Equation (16), and the field variables are h and $\overline{h}$. Then, the Lagrangian results are

$$L = \frac{\nabla h\nabla\overline{h}}{\left(h - \overline{h}\right)^2} \tag{21}$$

which, according to the variational principle (19), leads to the atmospheric field equations

$$\left(h-\overline{h}\right)\nabla^2 h = 2\nabla h \nabla h$$

$$\left(h-\overline{h}\right)\nabla^2 \overline{h} = 2\nabla \overline{h} \nabla \overline{h} \tag{22}$$

The solution of the first differentiable equation is written in the form

$$h = i\frac{\cosh\mu - e^{-i\alpha} sinh\mu}{\cosh\mu + e^{-i\alpha} sinh\mu} \tag{23}$$

with

$$\Delta\mu = 0 \tag{24}$$

and real and arbitrary α. Obviously, the variational principle (19) and the atmospheric field Equations (22) respectively describe a harmonic mapping between the Euclidean space of metric $\gamma_{\alpha\beta}$ and the upper half of the plane complex space—the Poincaré representation of the hyperbolic plane with the metric given by Equation (16), known as the invariant metric of the group $SL(2,R)$.

2.2. Coherences/Decoherences in Atmospheric Dynamics

Let us reconsider Equation (9) which represents the homographic action of the matrix:

$$\hat{M} = \begin{pmatrix} \alpha & \beta \\ \gamma & \delta \end{pmatrix} \tag{25}$$

The problem we want to solve is the following: find the relationship between the set of matrices $\hat{M}$ and a set of values of τ for which τ' remains constant (in this context, a constant τ' (derivative of the projective parameter) identifies a specific class of solutions where two atmospheric units evolve in such a way that their projective relationship remains geometrically fixed. This condition corresponds to projective synchronization and is used to define coherent dynamical relationships between regions). Geometrically, this means finding the set of points $(\alpha, \beta, \gamma, \delta)$ that uniquely corresponds to the parameter values τ.

Using Equation (9), our problem is solved by a Riccati differential equation that is obtained as a consequence of the constancy of τ [16], i.e.,

$$d\tau + \Omega_1 \tau^2 + \omega_2 \tau + \omega_3 = 0 \tag{26}$$

where we use the notations

$$\omega_1 = \frac{\gamma d\alpha - \alpha d\gamma}{\alpha\delta - \beta\gamma}, \omega_2 = \frac{\delta d\alpha - \alpha d\delta + \gamma d\beta - \beta d\gamma}{\alpha\delta - \beta\gamma}, \omega_3 = \frac{\delta d\beta - \beta d\delta}{\alpha\delta - \beta\gamma} \tag{27}$$

It is easy to verify that the metric

$$ds^2 = \frac{(\alpha d\delta + \delta d\alpha - \beta d\gamma - \gamma d\beta)^2}{4(\alpha\delta - \beta\gamma)^2} - \frac{d\alpha d\delta - d\beta d\gamma}{\alpha\delta - \beta\gamma} \tag{28}$$

is directly related to the discriminant of the quadratic polynomial from Equation (26):

$$ds^2 = \frac{1}{4}\left(\omega_2^2 - 4\omega_1\omega_2\right) \tag{29}$$

The three differential 1-forms from Equation (27) construct a co-frame at any point in the absolute space [16]. This co-frame allows us to translate the geometric properties of the absolute space into algebraic properties in correlation with differential Equation (26).

Most of these properties concern the motion on geodesics of the metric. In this case, differential 1-forms $\Omega_1, \Omega_2,$ and Ω_3 are exact differentials in the same parameter—the length of the arc of the geodesic, for example, s. Along these geodesics, Equation (26) transforms into an ordinary differential equation of the Riccati type (gauge of Riccati type):

$$\frac{d\tau}{ds} = P(\tau), \;\; P(\tau) = a_1\tau^2 + 2a_2\tau + a_3 \tag{30}$$

Here, parameters $a_1, a_2,$ and a_3 are constants that characterize a certain geodesic of the family. The most general solution of Equation (30) is obtained using the procedure from [16,17,29]. For this purpose, let us consider the roots of the quadratic polynomial be incorporated in the right-hand side of differential Equation (30), i.e.,

$$\tau_1 = -\frac{a_2}{a_1} + \frac{i}{a_1}\Delta, \;\; \tau_2 = -\frac{a_2}{a_1} - \frac{i}{a_1}\Delta, \; \Delta = a_1a_3 - a_2^2 \tag{31}$$

Making the transformation

$$y = \frac{\tau - \tau_1}{\tau - \tau_2} \tag{32}$$

it follows that y is a solution of the differential equation:

$$\dot{y} = 2i\Delta y, \;\; y(s) = y(0)e^{i\Delta s} \tag{33}$$

Now, if we conveniently express the initial condition y (0), we can give the general solution of Equation (30) by simply inverting transformation (32), with the result

$$\tau = \frac{\tau_1 + re^{2i\Delta(s-s_0)}\tau_2}{1 + re^{2i\Delta(s-s_0)}} \tag{34}$$

where r and s_0 are two real constants that characterize the solution. Using Equation (31), we can write these solutions in real terms, that is

$$y = -\frac{a_2}{a_1} + \frac{\Delta}{a_1}\left\{\frac{2r\sin[2\Delta(s-s_0)]}{1 + r^2 + 2r\cos[2\Delta(s-s_0)]} + i\frac{1-r^2}{1 + r^2 + 2r\cos[2\Delta(s-s_0)]}\right\} \tag{35}$$

which explains a modulation of Δ by a Stoler transformation [30], which leads us to the complex form of this parameter. Given the standard meaning of the Stoler transformation in the current context, it refers to the coherence/decoherence of atmospheric structural units in a given atmosphere (spatio-temporal correlation of local dynamics of atmospheric structural units within the global dynamics of a given atmosphere). Moreover, if we adopt the notation

$$r = \coth\mu \tag{36}$$

Equation (35) becomes

$$y = -\frac{a_2}{a_1} + \frac{\Delta}{a_1}\Psi \tag{37}$$

where Ψ has the expression

$$\Psi = -i\frac{\cosh\mu - e^{-2i\Delta(s-s_0)}\sinh\mu}{\cosh\mu + e^{2i\Delta(s-s_0)}\sinh\mu} \tag{38}$$

The meaning of the complex parameter was given in the previous section (see Equation (23)). For the moment, let us note that the coherence/decoherence process in the dynamics of atmospheric structural units is assimilated here to a process of modulation of Δ. More precisely, this process is a calibration of the difference between kinetic and potential energy—the classical definition of the Lagrangian—which leads this quantity to a perfect square. The physical significance of the perfect square Lagrangian is that it describes a fundamental physical unit (in our case, an atmospheric structural unit) within a complex system (in our case, the atmosphere), just as kinetic energy describes a free particle in space. Under these conditions, identifying Equation (23) with Equation (38) results in two-time scales, one corresponding to the time for the atmospheric structural unit and another corresponding to the time for the atmosphere. In general, by using Equation (35), various behaviors of the atmospheric structural units in the dynamics of atmosphere can be highlighted: period doubling, damped oscillations, quasi-periodicity, intermittency, chaos, etc., in accordance with [16].

In such a context, we present in Figure 2a,b the 3D and 2D dependences of Re $(ya_1 + a_2)$ by $s \equiv t$ for $\Delta \equiv \Omega_{max} = 3$ and r = 0.5, which mimic quasi-periodic-type behaviors. In our opinion, the tricellular model of general circulation of the atmosphere can be correlated with the quasi-periodicity modes of atmospheric dynamics.

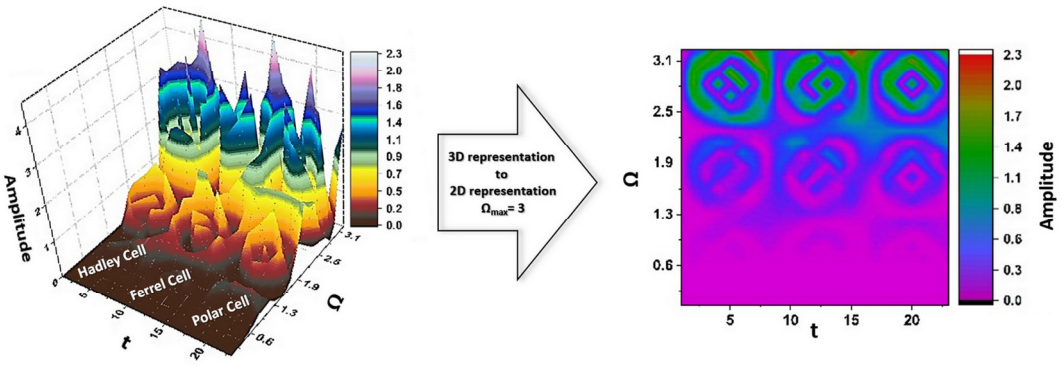

(**a**) (**b**)

Figure 2. Quasi-periodic-type behaviors in atmospheric dynamics: (**a**) 3D representation; (**b**) 2D representation and its correlation with the tricellular model of general circulation of the atmosphere.

In such a framework, the holographic behavior (the part reflects the whole and the whole reflects the part) appears as a universal property of the dynamics of structures in nature.

Let us consider the case

$$\mathrm{f}\left(\mathrm{f} - \frac{\partial \mathrm{u_g}}{\partial \mathrm{y}}\right) < 0 \tag{39}$$

Then, Equation (1) with the substitution becomes

$$\frac{1}{T^2} = f\left(\frac{\partial u_g}{\partial y} - f\right) \tag{40}$$

which takes the form

$$\frac{d^2\delta y}{dt^2} - \frac{1}{T^2}\delta y = 0 \tag{41}$$

and admits the general solution

$$\delta y = \delta y_0 ch\left(\frac{t - t_0}{T}\right) + V_0 T sh\left(\frac{t - t_0}{T}\right) \tag{42}$$

with $\delta y_0, V_0,$ and t_0 constants.

For $(t - t_0) \ll T$, Equation (42) describes inertial motion in Galilei's description:

$$\delta y \approx \delta y_0 + V_0(t - t_0) \tag{43}$$

For $(t - t_0) \gg T$, Equation (42) has a limit that we find based on the following mathematical procedure: we first derive the relation (42) with respect to time and eliminate δy_0 between the initial and the derived relation. This results in

$$\frac{d\delta y}{dt} = \frac{V_0}{ch\left(\frac{t-t_0}{T}\right)} + \frac{\delta y}{T} th\left(\frac{t - t_0}{T}\right) \tag{44}$$

This limit has the expression

$$\frac{d\delta y}{dt} = \frac{\delta y}{T} \tag{45}$$

Such a solution, for an ensemble of coherent atmospheric structural units, in our opinion, corresponds to atmospheric jets.

In Figure 3, we present the bifurcation diagram in the context of an inertially unstable atmosphere (where υ is the integration degree between atmospheric structural unity for a given atmosphere). In our paper, υ represents a structural index parameter that quantifies the relative spatial or dynamical position of an atmospheric unit within the system. It can encode variables such as latitude, vertical level, or local frequency class depending on the context of the synchronization analysis. Specifically, in the bifurcation diagrams, υ serves as a labeling axis for units or regions whose individual solutions are characterized by distinct projective parameters $\tau(t)$, allowing us to track the emergence of coherent regimes and identify zones of enhanced structural stability. Higher υ values correlate to polar cells if index υ is believed to be proportional to latitude, for instance, intermediate values map to the Ferrel cell. This lets υ encode spatial phase information in the synchronizing analysis.

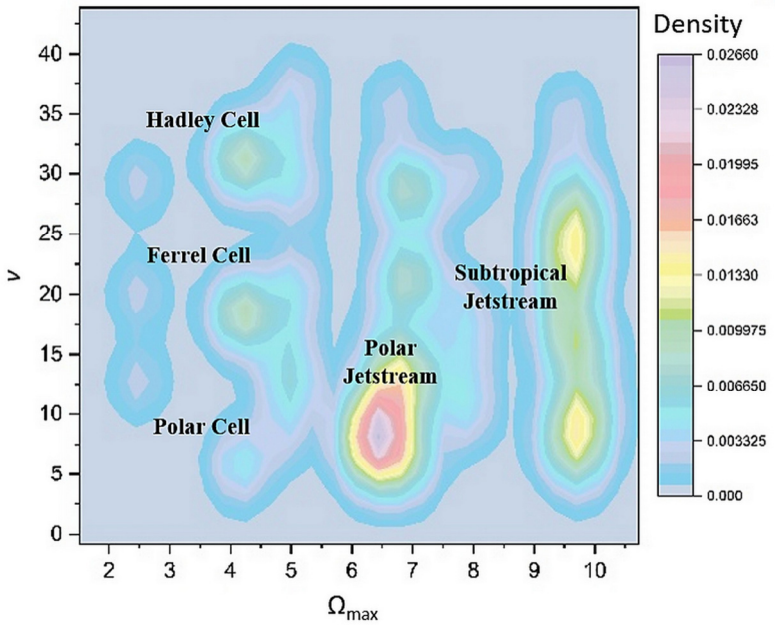

Figure 3. Tricellular model of the atmosphere correlated with the bifurcation map.

We also mention that this bifurcation diagram illustrates how coherent oscillatory regimes emerge as functions of the local frequency Ω and a structural or spatial parameter

ν. Each stability "island" in the diagram corresponds to a preferred natural frequency, associated with distinct atmospheric regimes such as the Hadley cell or the polar jet stream.

3. Results

The simplified dynamical model developed in this study captures the local response of a meridionally displaced air parcel within a rotating, sheared geostrophic flow—relevant to the onset of inertial instability. Although not derived from the full primitive-equation framework, the model retains the essential dynamics required to describe local imbalances between rotation and vorticity gradients. Reformulating the governing equation into a standard second-order linear form enables the construction of two independent solutions whose ratio defines a projective parameter governed by a Schwarzian differential equation—an equation invariant under homographic transformations.

This mathematical structure reveals a hidden symmetry associated with the SL(2,R) group, which governs geometric transformations of the solutions and leads to the emergence of projective synchronization. Physically, this implies that local atmospheric units may evolve coherently in phase space despite not being phase-identical. The resulting bifurcation patterns illustrate how preferred dynamical regimes emerge across a range of local frequencies and spatial conditions. The proposed framework thus complements classical linear theory by offering a symmetry-based perspective on how inertial instability can organize large-scale atmospheric structure.

4. Discussion

The present study offers a novel perspective on the nonlinear dynamics of atmospheric flows by revealing the role of a hidden symmetry in the context of inertial instability, starting from the single-particle model. This approach extends prior research in atmospheric dynamics by incorporating advanced mathematical methods from [16,23–25], providing a deeper understanding of the symmetry-driven mechanisms that govern the emergence and evolution of inertially unstable regimes.

Figure 1 demonstrates the atmospheric circulation triad (Hadley, Ferrel, and Polar cells) using Equivalent Potential Temperature cross-sections. In the interfacial zones, where vertical shear of geostrophic flow is maximized, conditions become conducive to inertial instability. Figures 2 and 3 illustrate how structural parameters (e.g., latitude-dependent index ν) modulate phase synchronization in atmospheric units. The nonlinear trajectories observed represent transitions between order and chaos—especially when phase locking or frequency entrainment occurs between different cells. The projected synchronization mechanism suggests a novel interpretation of the tricellular model, where atmospheric coherence emerges from group-theoretic invariants rather than strictly thermodynamic drivers.

The results suggest a potential link between the quasi-periodic modes observed in atmospheric circulation and the classical tricellular model of general circulation. Such an interpretation aligns with previous studies on nonlinear atmospheric dynamics while providing a new mathematical framework to describe both synchronization and coherence mechanisms within the system.

However, the model picked in this study has certain limitations. It is based on a simplified, differentiable equation of motion, which may not fully represent the complexity of real atmospheric phenomena (although it does capture essential nonlinear effects). Future research could explore more complex models, such as hydrodynamic or fractal-based approaches, to extend our results to a broader range of atmospheric conditions.

Despite these limitations, the results contribute to the field by demonstrating how hidden symmetries can be used to classify and predict different instability regimes in atmo-

spheric dynamics. This perspective advances our understanding of inertial instability and provides a mathematical framework for analyzing synchronization phenomena in complex geophysical systems. Furthermore, testing these theoretical results together with large-scale atmospheric data could refine our understanding of how nonlinear synchronization and coherence mechanisms influence weather patterns.

5. Conclusions

This study highlights the fundamental role of inertial instability in shaping atmospheric dynamics and momentum redistribution, emphasizing its nonlinear character. By extending the single-particle model and incorporating a hidden SL(2,R) symmetry of the equation of motion, we demonstrated that the synchronization of atmospheric structural units involves a temporal calibration in both frequency (SL(2,R) group-based) and phase (harmonic mappings).

Furthermore, the coherence of atmospheric dynamics is governed by Riccati-type gauges, leading to self-modulations via Stoler-type transformations. These mechanisms generate a variety of dynamic behaviors, including period doubling, damped oscillations, quasi-periodicity, intermittency, and chaos. Our findings suggest that the tricellular model of general atmospheric circulation can be correlated with the quasi-periodicity modes observed in inertially unstable regimes, providing a deeper understanding of large-scale flow structures.

Additionally, the introduction of hidden SL(2,R) symmetries and projective synchronization provides a compelling geometric paradigm to analyze phase-locked behavior among atmospheric structural units. This dual perspective—physical and geometric—enables a deeper understanding of the emergence of quasi-periodic regimes and chaotic transitions in planetary-scale circulation. Future studies should integrate moisture and latent heat processes into this symmetry-based framework and explore numerical simulations to validate the projected dynamics under real atmospheric conditions.

Author Contributions: Conceptualization, M.A., D.-C.B. and A.T.; methodology, M.A., D.-C.B. and A.T.; software, M.A.; validation, V.N., M.P.-L. and F.M.N.; formal analysis, M.A., D.-C.B., A.T., V.N., M.P.-L. and F.M.N.; investigation, D.-C.B. and A.T.; resources, M.A., D.-C.B., A.T., V.N., M.P.-L. and F.M.N.; data curation, M.A.; writing—original draft preparation, M.A., D.-C.B. and A.T.; writing—review and editing, A.T., V.N., M.P.-L. and F.M.N.; visualization, V.N., M.P.-L. and F.M.N.; supervision, M.A. and V.N.; project administration, D.-C.B., A.T., V.N., M.P.-L. and F.M.N.; funding acquisition, M.A., V.N., M.P.-L. and F.M.N. All authors have read and agreed to the published version of the manuscript.

Funding: This research received no external funding.

Data Availability Statement: The data presented in this study are available on request from the corresponding author due to their inclusion in ongoing research projects with related topics and approaches.

Conflicts of Interest: The authors declare no conflict of interest.

Appendix A. Derivation of Equation (1)

"[...] A parcel put into horizontal motion in a resting atmosphere with constant Coriolis parameter executes a circular trajectory in an anticyclonic sense. A generalization of this type of inertial motion to the case with a geostrophic mean zonal flow can be derived using a parcel argument similar to that used for the buoyancy oscillation." (Holton, 2004, page 204) [8].

If the flow corresponding to the zonal geostrophic basic state is considered with velocity u_g, and it is assumed that the particle displacement does not perturb the pressure field, then the approximate equations of motion between the initial position

$$\begin{cases} u_i = u_g \\ v_i = 0 \end{cases} \tag{A1}$$

and the final one

$$\begin{cases} u_f = u - u_g \\ v_f = v - 0 \end{cases} \tag{A2}$$

results in the system

$$\begin{cases} \frac{du}{dt} = f v_f \\ \frac{dv}{dt} = -f u_f = f(u_g - u) \end{cases} \tag{A3}$$

We consider a particle that moves along with the geostrophic flow corresponding to the basic state, which starts from position $y = y_0$. If the particle is transversely displaced to the current by a distance δy, a new zonal velocity $u(y_0 + \delta y)$ will result from the integration of Equation (A3)-first row.

$$\int_{u_{(y_0)}}^{u(y_0+\delta y)} \frac{du}{dt} = fv = f \int_{y_0}^{y_0+\delta y} \frac{dy}{dt} \tag{A4}$$

$$u(y_0 + \delta y) - u(y_0) = f\delta y \tag{A5}$$

$$u(y_0 + \delta y) = u(y_0) + f\delta y \tag{A6}$$

The geostrophic wind at the position $(y_0 + \delta y)$ can be approximated by

$$u_g(y_0 + \delta y) = u_g(y_0) + \frac{\partial u_g}{\partial y}\delta y \tag{A7}$$

Substituting (A6) and (A7) into (A3)-second row, we obtain

$$\frac{dv}{dt} = \frac{d^2}{dt^2}(\delta y) = f\left[u_g(y_0) + \frac{\partial u_g}{\partial y}\delta y - u(y_0) - f\delta y\right] \tag{A8}$$

$$\frac{d^2}{dt^2}(\delta y) = -f\left(f - \frac{\partial u_g}{\partial y}\right)\delta y \tag{A9}$$

It corresponds precisely to Equation (1) in this paper.

"Viewed in an inertial reference frame, instability results from an imbalance between the pressure gradient and inertial forces for a parcel displaced radially in an axisymmetric vortex. In the Northern Hemisphere, where f is positive, the flow is inertially stable provided that the absolute vorticity of the basic flow, is positive. In the Southern Hemisphere, however, inertial stability requires that the absolute vorticity be negative. Observations show that for extratropical synoptic scale systems the flow is always inertially stable, although near neutrality often occurs on the anticyclonic shear side of upper-level jet streaks. The occurrence of inertial instability over a large area would immediately trigger inertially unstable motions, which would mix the fluid laterally just as convection mixes it vertically, and reduce the shear until the absolute vorticity times f was again positive." (Holton, 2004, page 205–206) [8].

"[...] For typical atmospheric conditions, buoyancy tends to stabilize air parcels against vertical displacements, and rotation tends to stabilize parcels with respect to horizontal displacements. Instability with respect to vertical displacements is referred

to as hydrostatic (or simply, static) instability (see [8] Section 2.7.3). For an unsaturated atmosphere, static stability requires that the local buoyancy frequency squared be positive. Instability with respect to horizontal displacements, however, is referred to as inertial instability." (Holton, 2004, page 279) [8].

References

1. Spiridonov, V.; Ćurić, M. *General Circulation of the Atmosphere*; Springer: Cham, Switzerland, 2021; pp. 229–251. [CrossRef]
2. Arakawa, A. General circulation of the atmosphere. *Rev. Geophys.* **1975**, *13*, 668–680. [CrossRef]
3. Knox, J.A. Stratospheric Channels of Rossby Wave–Triggered Inertial Instability. 2005. Available online: https://ams.confex.com/ams/Cambridge/webprogram/Paper92879.html (accessed on 1 June 2025).
4. Met Office. Global Circulation Patterns. Available online: https://www.metoffice.gov.uk/weather/learn-about/weather/atmosphere/global-circulation-patterns (accessed on 1 February 2025).
5. Schneider, T. The general circulation of the atmosphere. *Annu. Rev. Earth Planet. Sci.* **2006**, *34*, 655–688. [CrossRef]
6. Martin, J.E. *Mid-Latitude Atmospheric Dynamics: A First Course*; Wiley: Hoboken, NJ, USA, 2006; p. 336, ISBN 978-0-470-86465-4.
7. EUMETSAT. EUMeTrain. Available online: https://eumetrain.org/ (accessed on 1 February 2025).
8. Holton, J.R. *An Introduction to Dynamic Meteorology*, 4th ed.; Elsevier: Amsterdam, The Netherlands, 2004; Volume 88, p. 535, ISBN 9780080470214.
9. Vallis, G.K. *Atmospheric and Oceanic Fluid Dynamics*, 2nd ed.; Cambridge University Press: Cambridge, UK, 2017.
10. Dunkerton, T.J. *Gravity Waves in the Atmosphere: Instability, Saturation, and Transport*; Defense Technical Information Center: Bellevue, WA, USA, 1995.
11. Pedlosky, J. *Geophysical Fluid Dynamics*, 2nd ed.; Springer Nature: Dordrecht, The Netherlands, 1987. [CrossRef]
12. Bluestein, H.B. Volume I: Principles of Kinematics and Dynamics. In *Synoptic-Dynamic Meteorology in Midlatitudes*; Oxford University Press: Oxford, UK, 1992; p. 448. ISBN 9780195062670.
13. Shimizu, M.H.; de Albuquerque Cavalcanti, I.F. Variability patterns of Rossby wave source. *Clim. Dyn.* **2011**, *37*, 441–454. [CrossRef]
14. Marras, S.; Kelly, J.F.; Moragues, M.; Müller, A.; Kopera, M.A.; Vázquez, M.; Giraldo, F.X.; Houzeaux, G.; Jorba, O. A review of element-based galerkin methods for numerical weather prediction: Finite elements, spectral elements, and discontinuous galerkin. *Arch. Comput. Methods Eng.* **2015**, *23*, 673–722. [CrossRef]
15. Kalashnik, M.V.; Kurgansky, M.V.; Chkhetiani, O.G. Baroclinic instability in geophysical fluid dynamics. *Physics-Uspekhi* **2022**, *65*, 1039–1070. [CrossRef]
16. Agop, M.; Irimiciuc, S.A. *Multifractal Theory of Motion: From Small to Large Scales*; Springer Nature: Singapore, 2024; p. 174.
17. Fortuna, E.; Frigerio, R.; Pardini, R. *Projective Geometry: Solved Problems and Theory Review*; Springer: Berlin/Heidelberg, Germany, 2016; Volume 104.
18. Bordag, L.A.; Dryuma, V.S. Investigation of dynamical systems using tools of the theory of invariants and projective geometry. *Discret. Contin. Dyn. Syst.* **1997**, *48*, 725–743. [CrossRef]
19. Rebelo, R.; Winternitz, P. Invariant difference schemes and their application to *sl*(2, R) invariant ordinary differential equations. *J. Phys. A Math. Theor.* **2009**, *42*, 454016. [CrossRef]
20. Arkani-Hamed, N.; Bai, Y.; Lam, T. Positive Geometries and Canonical Forms. *J. High Energy Phys.* **2017**, *2017*, 39. [CrossRef]
21. Olver, P.J. *Applications of Lie Groups to Differential Equations*; Springer Science & Business Media: Berlin/Heidelberg, Germany, 1993; Volume 107.
22. Bluman, G.W.; Kumei, S. *Symmetries and Differential Equations*; Springer Science & Business Media: Berlin/Heidelberg, Germany, 2013; Volume 81.
23. Tesloianu, N.D.; Nedelciuc, I.; Ghizdovat, V.; Agop, M.; Ursulescu, C.L. A fractal physics explanation for acute thrombotic occlusion in an apparently healthy coronary artery. *Anatol. J. Cardiol.* **2017**, *18*, 155–157. [CrossRef] [PubMed]
24. Mazilu, N.; Ghizdovat, V.; Agop, M. Role of surface gauging in extended particle interactions: The case for spin. *Eur. Phys. J. Plus* **2016**, *131*, 139. [CrossRef]
25. Mazilu, N.; Agop, M.; Gatu, I.; Iacob, D.D.; Ghizdovăt, V. From Kepler problem to skyrmions. *Mod. Phys. Lett. B* **2016**, *30*, 1650153. [CrossRef]
26. Dasgupta, B.; Raffelt, G.G.; Tamborra, I. Triggering collective oscillations by three-flavor effects. *Phys. Rev. D* **2010**, *81*, 073004. [CrossRef]
27. Akhiezer, A.I.; Akhiezer, I.A.; Polovin, R.V. *Collective Oscillations in a Plasma: International Series of Monographs in Natural philosophy*; Elsevier: Amsterdam, The Netherlands, 2017; Volume 7.
28. Artemenko, S.N.; Volkov, A.F. Electric fields and collective oscillations in superconductors. *Sov. Phys. Uspekhi* **1979**, *22*, 295–310. [CrossRef]

29. Cariñena, J.F.; Ramos, A. Integrability of the Riccati equation from a group-theoretical viewpoint. *Int. J. Mod. Phys. A* **1999**, *14*, 1935–1951. [CrossRef]
30. Stoler, D. Generalized Coherent States. *Phys. Rev. D* **1971**, *4*, 2309. [CrossRef]